NUMERICAL SIMULATION OF NON-UNIFORM GAS DIFFUSION LAYER POROSITY EFFECT ON POLYMER ELECTROLYTE MEMBRANE FUEL CELL PERFORMANCE

R. Roshandel and B. Farhanieh*

Department of Mechanical Engineering, Sharif University of Technology
P.O. Box 11365-9567, Tehran, Iran
roshandel@mech.sharif.edu - bifa@sharif.edu

*Corresponding Author

(**Received: Novamber 21, 2006 – Accepted in Revised Form: May 31, 2007)**

Abstract Gas diffusion layers are essential components of proton exchange membrane fuel cell since the reactants should pass through these layers. Mass transport in these layers is highly dependent on porosity. Many of simulations have assumed, for simplicity, the porosity of GDL is constant, but in practice, there is a considerable variation in porosity along gas diffusion layers. In the present study the porosity variation in GDL is calculated by considering the applied pressure and the amount of water generated in the cell. A two dimensional mathematical model is developed to investigate the effect of stack compression and water generation on porosity of GDL and cell performance. The validity of the model is assessed by comparing the computed results with experimental data. The results show that when the electrical current density is low, the porosity variation in the gas diffusion layer has no significant influence on the level of polarization whereas at higher current density the influence is very significant. It is also shown that, the electrical current has a sharp gradient across the catalyst layer. Therefore, the better cell performance could be achieved by adding a certain amount of catalyst loading to each electrode, with respect to the reactant concentration.

Keywords Simulation, Polymer Electrolyte, Fuel Cell, Gas Diffusion Layer, Porosity

چکیده لایه های نفوذ گاز یکی از ضروری ترین قسمتهای پیل سوختی هستند. مهمترین وظیفه آنها انتقال گاز های واکنش دهنده است. انتقال جرم در این لایه ها به میزان تخلخل بستگی دارد. در بسیاری از کارهای شبیه سازی انجام شده، تخلخل این لایه ها ثابت فرض شده است. اما در واقع به دلیل جمع شدن آب و فشار مونتاژ، تغییرات زیادی در تخلخل این لایه ها به وجود می‌آید. غیر یکنواختی تخلخل لایه های نفوذ گازی موجب می‌شود که مواد تشکیل دهنده به صورت نامنظم روی لایه های کاتالیستی واکنش دهند و به این ترتیب جریان الکتریکی تولید شده یکنواخت نباشد. در این مقاله تاثیر غیر یکنواختی تخلخل ناشی از تجمع آب تولید شده در پیل و فشار مونتاژ اجزاء پیل بر کارایی پیل مورد بررسی قرار گرفته است. برای اطمینان از صحت شبیه سازی انجام شده، منحنی پلاریزاسیون با نتایج تجربی مقایسه گردیده است. نتایج شبیه سازی نشان دهنده تاثیر غیر یکنواختی تخلخل در لایه های نفوذ گاز بر جریان های الکتریکی بالا است به طوری که جریان الکتریکی تولید شده در سطح لایه های کاتالیستی کاملاً غیر یکنواخت می‌باشد. برای کاهش تاثیرات عدم یکنواختی جریان الکتریکی، استفاده از لایه های کاتالیستی سوار شده بر هر الکترود پیشنهاد می‌شود.

1. INTRODUCTION

Fuel cells convert the chemical energy of hydrogen and oxygen into electricity. Their high efficiency and low emissions have made them a very suitable power system for the next generation of vehicular application as well as small stationary power plants. Fuel cells are usually classified by the nature of electrolyte they use. Polymer electrolyte membrane (PEM) fuel cell systems are considered to be promising and environmentally friendly power sources. This is due to the attributes of high

energy density at low operating temperatures, good performance in intermittent operation, zero emission, quick start up capacity, and minimal problems from components corrosion and electrolyte leakage [1,2].

The properties of the diffusion layer effects the optimum performance of the catalyst and electrode [3]. These layers are porous to allow for distribution of the gases to unexposed areas of the flow channel and for complete utilization of the electrode area. The electrical conductivity of these layers could affect the transport of electrons to the current collector from the electrode.

The development of a theoretical model of the PEM fuel cell as well as corresponding analyses, are crucial to gain a good understanding of the effect of operating conditions on the cell potential. Most of the studies in this area have assumed simplicity constant porosity of the GDL [4-8]. This, however, can not reflect the importance of GDL porosity on fuel cell performance. The hydrophobicity of the diffusion layers may interact with the amount of water available for hydration at the membrane. The catalyst layer and portion of the gas diffusion layer are typically impregnated with hydrophobic media like Teflon to improve water transport. The thickness and porosity of the gas diffusion layers can also change due to applied compression. These layers can be porous carbon cloths or paper coated with polytetrafluoroethylene (PTFE). Although it has been recognized that the performance of the fuel cell can be significantly influenced due to the porosity variation [9-15], systematical studies are still rarely reported in the open literature.

Gurau et al. [16] considered the non-uniformity of the porosity of the gas diffusion layers by developing a one-dimensional half-cell model in which the concept of the effective porosity was employed to account for the fact that the pores may be partially filled with liquid water. Chu et al. [17] investigated the effects of non-uniform porosity on fuel cell performance in terms of physical parameters such as oxygen consumption, current density, power density, etc. The non-uniformity of the porosity was accounted for by four different continuous functions of position, each of which had a different averaged value of porosity and a different type of distribution across the diffusion layers. Lee et al. [18] experimentally studied the effects of porosity change on the performance of the fuel cell due to the compression applied onto the GDL. Z. Zhan et al. [19] investigated the effect of porosity distribution variation on the liquid water flux through gas diffusion layers of PEM fuel cells. S. Lee et al. [20] analyzed the effect of assembly pressure on fuel cell performance. W. Yan et al. [21] developed a transient model of reactant gas transport based on GDL morphology, geometry and porosity and H. Lin et al [22] presented the method to optimize cell performance in term of these parameters. A comprehensive review of the mathematical modeling of proton exchange membrane fuel cells is provided in W. Tao et al. [23], C. Min et al. [24] and L. Ma et al. [25].

In the present study, fuel cell performance is investigated by considering the effects of porosity variation distribution in gas diffusion layers. The effect of compression of the electrodes on the solid landing area and the water generated at cathode side of GDL are both considered in expressing the variation of porosity distribution.

2. MATHEMATICAL MODEL

The operation principle of a PEM fuel cell is presented in Figure 1. Humidified air enters the cathode channel and hydrogen diffuses through the anode diffusion layer towards the catalyst, where each hydrogen molecule splits up into two hydrogen protons and two electrons according to:

$$2H_2 \rightarrow 4H^+ + 4e^- \quad (1)$$

The protons migrate through the membrane and the electrons travel through the conductive diffusion layer and an external circuit where they produced electric work (Figure 1). On the cathode side the oxygen diffuses through the diffusion layer, splits up at the catalyst layer surface and reacts with the protons and electrons to form water:

$$O_2 + 4e^- + 4H^+ \rightarrow 2H_2O \quad (2)$$

From above, it can be seen that the overall reaction

in a PEM fuel cell can be written as:

$$2H_2 + O_2 \rightarrow 2H_2O \quad (3)$$

2.1. Gas Diffusion Layer Modeling The gas diffusion layer does much more than diffuse the gas. It forms an electrical connection between the catalyst layer and the bipolar plate, or other current collectors. In addition, it carries the product water away from the electrolyte surface, and also forms a protective layer over a very thin layer of catalyst. They are usually made of a porous carbon paper or carbon cloth, typically 100 to 300 microns thick. The gas diffusion layer also assists in water management during the operation of the fuel cell. Too little or too much water can cause the cell to cease operations.

The correct backing material allows the right amount of water vapor to reach the membrane and keep it humidified. Therefore, it is important to investigate and analyze the effect of reactant distribution in this layer on the fuel cell performance. A cross sectional view through a GDL is depicted in Figure 2.

The upper boundary (I,II) represents the interface between the GDL and either the solid graphite plate or an open Gas-filled flow channel. The lower boundary (IV) corresponds to the catalyst layer separating the GDL and the Polymer electrolyte membrane. Single-phase flow in porous media is typically modeled using Darcy's law.

$$\vec{U}_g = -\frac{K}{\mu}\nabla P \quad (4)$$

In this equation the averaged velocity is related to pressure gradient. The equation of continuum for the reactant gas is:

$$\nabla.\left(\rho_g \vec{U}_g\right) = 0 \quad (5)$$

Where $\vec{U}$ is a mass-averaged velocity. The conservation law for the reactant concentration takes the form:

$$\nabla.\left(C_g \vec{U}_g + D_g^{eff}\,\rho_g \nabla\left(\frac{C_g}{\rho_g}\right)\right) = 0 \quad (6)$$

The diffusive flux is given by Fick's law, which states that the flux of one component relative to the molar average velocity is proportional to the gradient in mole fraction via:

$$\vec{N}_g = -\rho_g D_g^{eff} \nabla\left(\frac{C_g}{\rho_g}\right) \quad (7)$$

Where N_g is the molar diffusive flux(measured relative to the mass-averaged velocity) and D is the coefficient of diffusion and is related to the fluid properties and the porosity of the gas diffusion

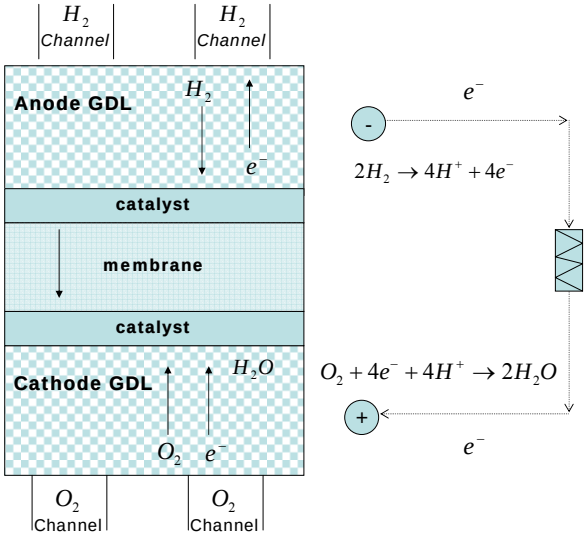

Figure 1. Operating scheme of a PEM fuel cell.

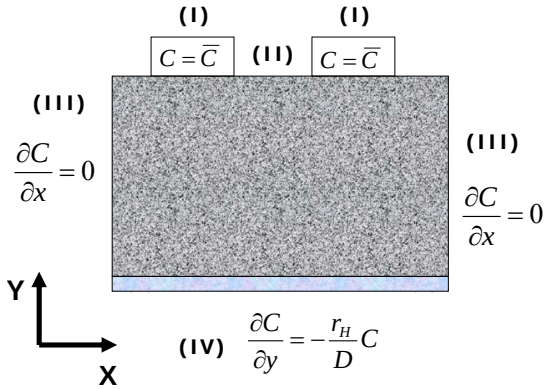

Figure 2. Cross-section of the gas diffusion layer and gas flow channels.

layer. In isotropic porous media, the dependence of the diffusion coefficient on porosity is often approximated using Bruggeman's correction [26]:

$$D_g^{eff} = D_g \varepsilon_g^{1.5} \quad (8)$$

This relates the effective diffusivity in the porous medium to that of a free gas. In an ideal gas mixture, the pressure depends linearly on the mixture concentration (and hence the density) via the ideal gas law:

$$P = C_g RT = \frac{\rho RT}{m} \quad (9)$$

Thus, the Darcy equation for gas reactant in isothermal condition becomes:

$$\vec{U}_g = -\frac{KRT}{\mu} \nabla C_g \quad (10)$$

The boundary consists of four distinct components, labeled I-IV in Figure b2. The boundary conditions on each of the four sections are obtained as follows [27]:

- The permeable boundary is where the mixture concentration inside the GDL is immediately taken to be identical to that in the channel.

$$C_g = \overline{C}_g \quad (11)$$

That is, the pressure is assumed to be uniform throughout the depth of the channel. Further it is assumed that diffusive flux of the component across the channel/GDL interface is proportional to the difference in the concentration on either side.

$$N_g = r_0\left(\overline{C}_g - C_g\right) \quad (12)$$

- The impermeable boundary between the graphite plate and the GDL where no-flow conditions on the vertical component of fluxes are imposed.

$$N = 0$$
$$\frac{\partial C_g}{\partial y} = 0 \quad (13)$$

- The open side boundaries, where a periodic solution in x-direction is assumed.

- The boundary conditions at the permeable boundary between the catalyst and GDL are:

$$N_g = r_H C_g \quad (14)$$

$$\frac{\partial C_g}{\partial y} = -\frac{r_H}{D_g^{eff}} C_g \quad (15)$$

The mass transfer coefficient r_H models the reactions and electrochemistry taking place in the catalyst region. The Pt catalyst is considered to be applied in the catalyst layer, In practice, the mass transfer coefficient r_H is tuned so as to match net flux to experimental values [27]. Jeng et al. [28] provided a relation for r_H as:

$$r_H = \frac{A_v i_0 l_c \exp\left(\frac{F\eta_{act}}{RT}\right)}{4F\varepsilon_c^{1.5} C^{ref}} \quad (16)$$

Therefore, the r_H value can be evaluated for the given overpotential and the physical parameter and properties according to [28].

2.2. Porosity Variation Due to Compression Most of the models have assumed the simplicity for the porosity of the GDL is constant. This, however, may not reflect the importance of GDL porosity on fuel cell performance. Any change in the composition or the morphology of the GDL can lead to a substantial influence on fuel cell performance owing to a porosity change. In order to seal the fuel cell against any gas leakages, the gas diffusion layer and bipolar plate are bolted together under significant pressure [27]. Another reason for bolting the fuel cell together is to reduce electrical contact resistance. Compressing the GDL reduces the porosity over the landing area, which in turn decreases the overall flux of reactant to the catalyst layer, particularly above the landing area (Figure 3). The effect of compression on the porosity variation is considered by allowing the porosity to vary as a function of x. Since the thickness of the GDL is considerably

small, the variation in the porosity, due to compression in the Y direction, is negligible. Based on the best approximation theory for unknown functions; the best choice for this approximation function is a polynomial in the bases of orthogonal functions which are the solutions of the Sturm-Liouville theory. The most famous orthogonal functions are the Fourier functions (sin(x) and cos(x)) and the Lagrange polynomials. Therefore, using a composition of the functions in the form of $\sin^{2n}x$ which is appropriately scaled and translated, a function for the variation of porosity across the gas diffusion layer could be obtained [27].

$$\varepsilon_g^{comp}(x) = \varepsilon_g^0\left(\sum_n A_n \sin^{2n} x\right) \quad (17)$$

Where ε^0 is initial porosity and ε^{comp} is the porosity of the gas diffusion layer after the compression process. A_n coefficients are selected as a function of compression pressure based on experimental results of Lee et al. [18]. The assembly pressure increased from 125 to 150 in. lb_f/bolts.

2.3. Porosity Variation Due to Water Management It is clear from the description of the proton exchange membrane that there must be sufficient water content in the polymer electrolyte, otherwise the conductivity decreases. However, there must not be so much water that blocking occurs in the pores of the gas diffusion layer. Thus the presence of water generated in the GDL during fuel cell operation can change the effective porosity [17]. To consider the non-uniformity of the porosity of the GDL caused by the presence of water, all flow rates related to the different phenomena should be determined. Then the effective porosity can be specified by considering the presence of additional water amounts in the fuel cell. Figure 4 outlines the water flow inside the cell.

2.3.1. Water input Water entering the cell due to the fuel and oxidant humidification:

$$w_-^{hum} = \frac{I}{2F}\zeta_- \frac{x_{w-}^{hum}}{1 - x_{w-}^{hum}} \quad (18)$$

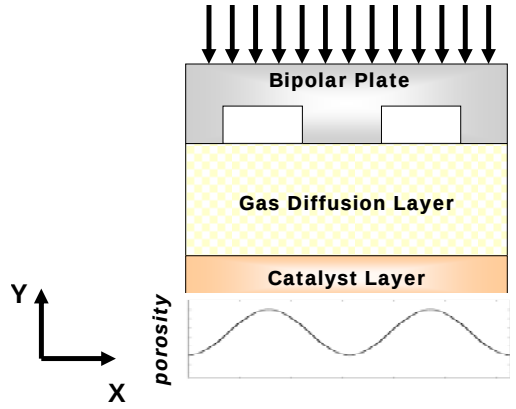

Figure 3. Effect of compression of gas diffusion layer porosity.

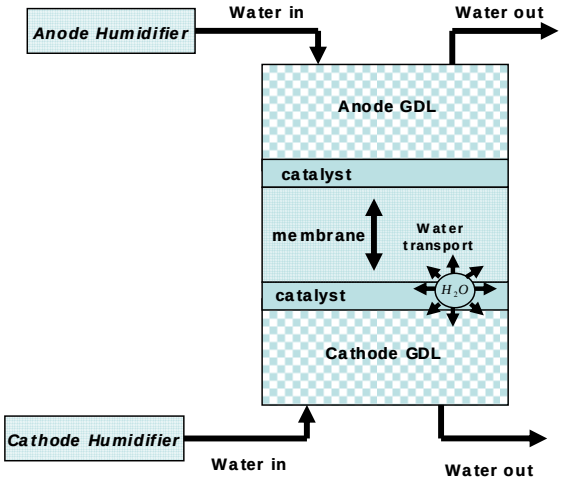

Figure 4. Schematic of water flows in a PEM fuel cell.

$$w_+^{hum} = \frac{I}{4F}\zeta_+ \frac{x_{w+}^{hum}}{1 - x_{w+}^{hum}}\left(1 + \frac{x_{N_2}^0}{x_{O_2}^0}\right) \quad (19)$$

The mole fraction of water corresponding to humidification conditions (x_-^{hum}, x_+^{hum}) can be determined by considering the humidification temperature.

2.3.2. Water production Water produced in the cell (on the cathode side) from the electrochemical reaction:

$$w^{el} = \frac{I}{2F} \tag{20}$$

2.3.3. Water transport Water transport in the membrane which depends on the electro-osmotic transport associated with the flow of the H^+ protons, and the diffusive transport due to a pressure gradient in the membrane [4]. The velocity U_m is defined as the velocity of liquid water in the pores of the membrane phase. In accordance with Schlögl equation, U_m is related to the hydraulic pressure and the potential gradients:

$$U_m = \varepsilon_m \left(\frac{k_\varphi}{\mu_w} C_{H^+} F\nabla\phi - \frac{k_h}{\mu_w} \nabla P \right) \tag{21}$$

Bernardi and Verbrugge [4,7] presented a complete discussion on water velocity in the pores of membranes. The first term on the right hand side of Equation 21 is the component of the membrane velocity that is due to the potential driving force, and the second term is the flow component which is due to the pressure gradient through the membrane. The membrane is assumed to be fully humidified so that the electronic conductivity is constant and according to references such as Bernardi and Verbrugge [4,7], Maggio et al. [29] and Berning et al. [30], no diffusive terms have to be considered for liquid water flux. The membrane water transport ratio can be calculated from [7]:

$$\xi = \varepsilon_w^m F \frac{\delta}{I} U_m \tag{22}$$

The water transport in the membrane pores can be determined using the following expression:

$$w^{tr} = \frac{I}{F} \xi \tag{23}$$

2.3.4. Water outlet The water outlet from the fuel cell is calculated using

$$w_-^{out} = \frac{I}{2F} \left(\zeta_- - 1 \right) \frac{x_{w-}^{sat}}{1 - x_{w-}^{sat}} \tag{24}$$

$$w_+^{out} = \frac{I}{4F} \left[\zeta_+ \left(1 + \frac{x_{N_2}^0}{x_{O_2}^0} \right) - 1 \right] \frac{x_{w+}^{sat}}{1 - x_{w+}^{sat}} \tag{25}$$

The water balance is expressed by the following relationships:

$$M_- = w_-^{hum} + w^{tr} - w_-^{out} \tag{26}$$

$$M_+ = w_+^{hum} + w^{el} - w^{tr} - w_+^{out} \tag{27}$$

As mentioned earlier, the average effective porosity of the GDL should be significantly lower than the natural porosity of the carbon cloth electrode. The reason is a noticeable "partial flooding" of the cathode by the produced liquid water which decreases the effective porosity of the gas diffusion layer. In the mathematical model presented in Springer et al. [31], the effective porosity could be adjusted and was considered to decrease in proportion to the rate of water production at the cathode. To obtain reliable value of the effective porosities corresponding to a given fuel cell, Maggio et al. [29] was forced to realize a simultaneous fitting of several polarization curves of the cell recorded under different operative conditions. Their approach, allows direct calculation of the effective porosity through Equation 28

$$M_+ > 0 \text{ if } \varepsilon^{hum} = \varepsilon^0 \left(1 - \frac{M_+}{M_{max}} \right) \tag{28}$$

2.4. The Effect of Porosity on Fuel Cell Performance The performance of a PEM fuel cell can be illustrated by a voltage vs. current density plot, or polarization curve. The polarization curve can be divided into three regions characterized by activation overpotential, Ohmic overpotential, and concentration overpotential. Therefore, the operational fuel cell voltage can be written as:

$$V = V_{OCV} - \eta_{act} - \eta_{ohm} - \eta_{dif} \tag{29}$$

2.4.1. Activation overpotential In the activation overpotential region, the dominant

source of losses is due to resistance to electrochemical reactions. These losses are also referred to as activation losses, occurring when slow electrochemical reactions are driven from equilibrium in order to produce electric currents [7]. The activation overpotential can be calculated from:

$$\eta_{act} = \frac{RT}{F}\ln\left(\frac{I}{I_0}\right) \quad (30)$$

2.4.2. Ohmic overpotential The Ohmic overpotential from electronic and ionic resistance in the cell is the most significant source of performance degradation in medium current density while in low current density activation overpotential and in high current density diffusion overpotential is more significant. The Ohmic losses in the GDL can be calculated as:

$$\eta_{ohm,g} = \frac{I}{\sigma} l_g \quad (31)$$

The membrane loss is related to the fact that an electric field is necessary in order to maintain the motion of the hydrogen protons through the membrane. It can be shown that this loss obeys Ohm's law [32]

$$\eta_{ohm,m} = \frac{I}{\kappa} l_m \quad (32)$$

Bernardi and Verbrugge [4] developed the following theoretical expression for the electric conductivity of the membrane:

$$\kappa = \frac{F^2}{RT} z_f D_{H_+} C_{H_+} \quad (33)$$

The expression leads however to an over-estimation of the conductivity compared to experimentally determined results, which range between 0.03 and 0.06 S/cm for an ambient humidity of 100 % [33]. In this work, a value of 0.068 was taken for the ionic conductivity of the membrane, which agree with the value used by Springer et al. [31]

2.4.3. Concentration (diffusion) overpotential In the concentration overpotential region, losses due to mass transport limitations are dominant. Concentration overpotential occurs when the chemical reaction is limited by the rate of which reactants can be supplied. This lack of reactant slows the electrochemical reaction, resulting in a lower cell potential. This amount can be calculated by [29]:

$$\eta_{dif} = \omega T I \ln\left(\frac{I_{lim}}{I_{lim} - I}\right) \quad (34)$$

Where I_{lim} is the limiting current density that is affected by additional water amount and effective porosity of the gas diffusion layer in a PEM fuel cell. ω is an experimental factor and evaluated from extrapolation of data reported in [34]. The value of this factor is given in Table 1, according to Maggio [29]. The limiting current density is a measure of the maximum by which a reactant can be supplied to an electrode. The rate of mass transport to an electrode surface in many cases can be described by Ficks's Law [3]:

$$I = \frac{nFD_g^{eff}\left(\overline{C} - C_c\right)}{l_g} \quad (35)$$

Where D is an effective diffusion coefficient of the reactant species. $\overline{C}$ is channel concentration and C_c is reactant concentration in the catalyst layer. The limiting current density occurs when $C_c = 0$

$$I_{lim} = \frac{nFD_g^{eff}\overline{C}}{l_g} \quad (36)$$

3. RESULTS AND DISCUSSION

Accuracy tests were performed on the numerical procedure, particularly to study the effect of the grid fineness on the solution. Comparison of the mole fraction along the channel under various grid sizes were made and presented in Figure 5. The results show that by increasing the fineness of the grid no significant changes appear in the mole fraction distribution. The final computations were performed with 40×40 grid points to maintain relatively

TABLE 1. Cell Operating Condition.

Description	Symbol	Value
Cell Temperature	T	346.15°K
Pressure at the anode Side	p_a	3 atm
Pressure at the Cathode Side	P_c	5 atm
Anode Stoichiometry	ζ_a	1.2
Cathode Stoichiometry	ζ_c	3
Anode Humidifier Temperature	T_a^{hum}	358°K
Cathode Humidifier Temperature	T_c^{hum}	353°K

moderate computing times in the final calculations. It is clear from Figure 5 that the difference between mole fractions in the two last grid sizes is less than one percent. To assess the accuracy of the mathematical model, the comparison of the computed polarization curve for air and oxygen with the experimental data of Maggio et al. [29] is presented in Figure 6. As seen from this figure, the results of the present computations agree well with the experimental data. In the high current density (more than 0.5 A/cm^2), due to more water generation, the mass transport losses are more important and affects the polarization curve but in the first two cases, the decreases of porosity are not considered. Therefore, significant deviation above a current density of 0.5 A/cm2 for the first two curves is due to ignoring the increases of mass transport overpotential.

The set of governing differential equations (Equations 4-10) with given boundary conditions (Equations 11-14) were discretized with the Finite Volume method and solved numerically by iterative algorithm.

To investigate the effect of porosity on gas reactant distribution in an anode and cathode gas diffusion layer the porosity distribution in the first step is considered to be constant. In Figure 7 the reactant mole fraction is presented. The cathode stream consists of 21 % oxygen and 69 % nitrogen, the remaining 10 % of the gas is water vapor. The mole fraction plot shows that gas concentration decreases from channel to membrane as the reactant is consumed. However, the reactant concentrations in the GDL/membrane interface as well as the electrical current density are both uniform. The average of electrical current density is 0.61 A/cm^2. The produced current density is obtained by the well known Butler-Volmer equation.

Figure 8 presents the reactant distribution in GDL when porosity is considered as a function of compression pressure. This function is provided in Equation 17. In this case, due to the compression the porosity decreases especially under the landing area. This causes a decrease in overall reactant flux to the catalyst layer particularly under the landing areas and thus creating a more non-uniformity in the gas diffusion layer. Therefore, the variation of the electrical current increases across the electrodes. It means that some of the catalyst particles, especially under the landing area remain unused and the average electrical current density reduces to 0.47 A/cm^2 (~23 % less!)

Another source of variation in the GDL's porosity is presence of water in the layers. If too much water is present, flooding may occur resulting in the pores of the gas diffuser filled with liquid water, which blocks the transport of reactant to the reaction site in the cathode side. It is shown in Figure 9 that the water decreases the effective porosity of GDL and which in turn causes the reduction in the oxygen concentration in GDL/Membrane interfaces. In fact the porosity in the diffusion layer decreases from the initial 74 % to 55 % considering the blockage of the pores by water.

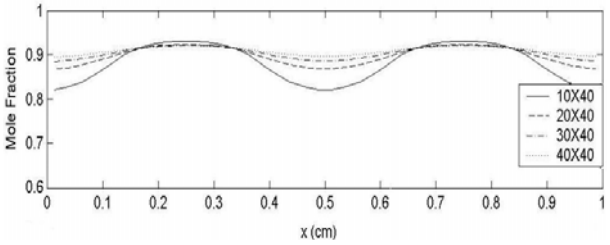

Figure 5. Comparison of the oxygen mole fraction along the channel under various grid sizes.

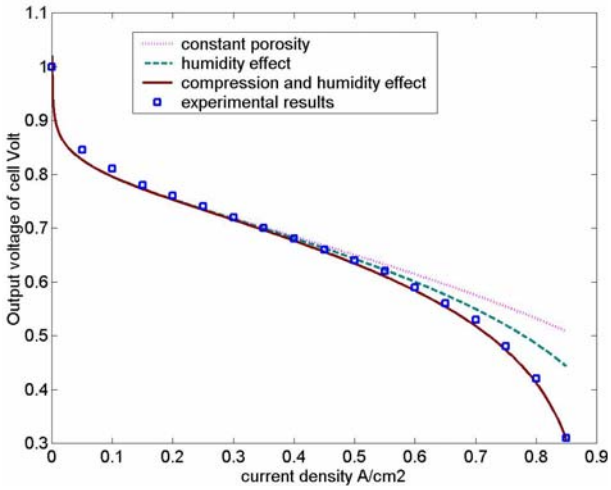

Figure 6. Polarization curve comparison between model and experimental results (Experimental data taken from Maggio et al.).

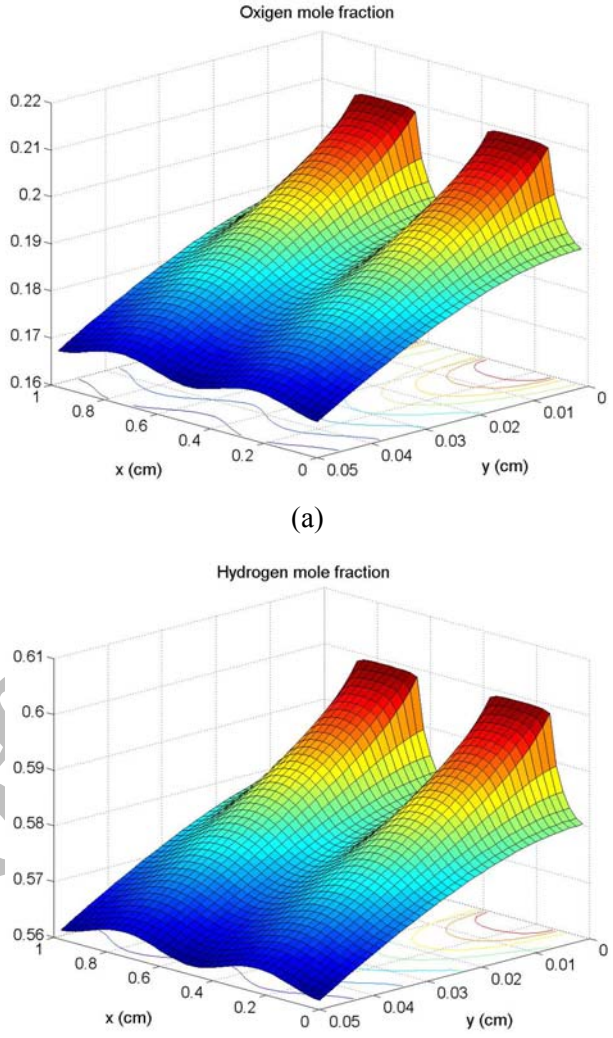

Figure 7. Reactant mole fraction in gas diffusion layer with constant porosity distribution, (a) Cathode and (b) Anode side of cell.

Figure 10 shows the electrical current density in electrodes corresponding to reactant concentrations. It can be observed that compression pressure affects the electrical current distribution along the electrodes and makes peaks in the electrode current densities.

As already mentioned, porosity variation changes the limiting current density and so the diffusion overpotential increases. However, the potential drop related to the diffusion overpotential appears to be too sharp compared with other overpotentials.

Figure 11 presents the contributions of the relative share of the calculated overpotential corresponding to different porosity distributions. It can be observed that diffusion overpotential increases from 11 % to 30 % when average effective porosity deceases due to the compression pressure and presence of liquid water in gas diffusion layers.

As mentioned earlier, due to the compression and water presence in GDL, the porosity decreases especially under the landing area. This causes a decrease in overall reactant flux to the catalyst layer particularly under the landing areas and thus creating more non-uniformity in the gas diffusion

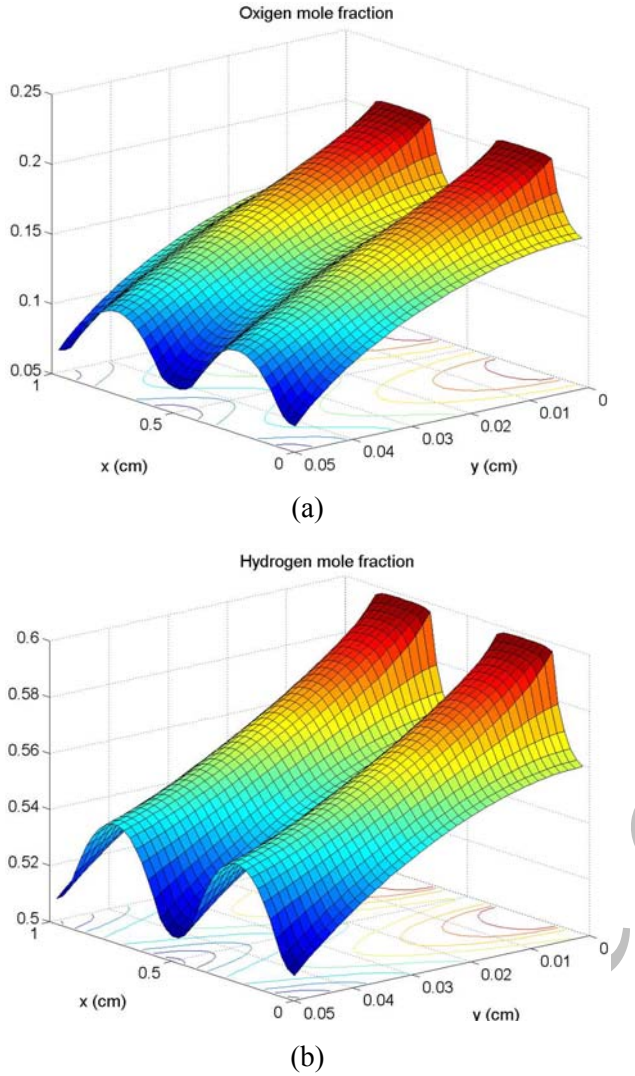

Figure 8. Reactant mole fraction in gas diffusion layer with consideration of compression effect on porosity of GDL, (a) Cathode and (b) Anode side of cell.

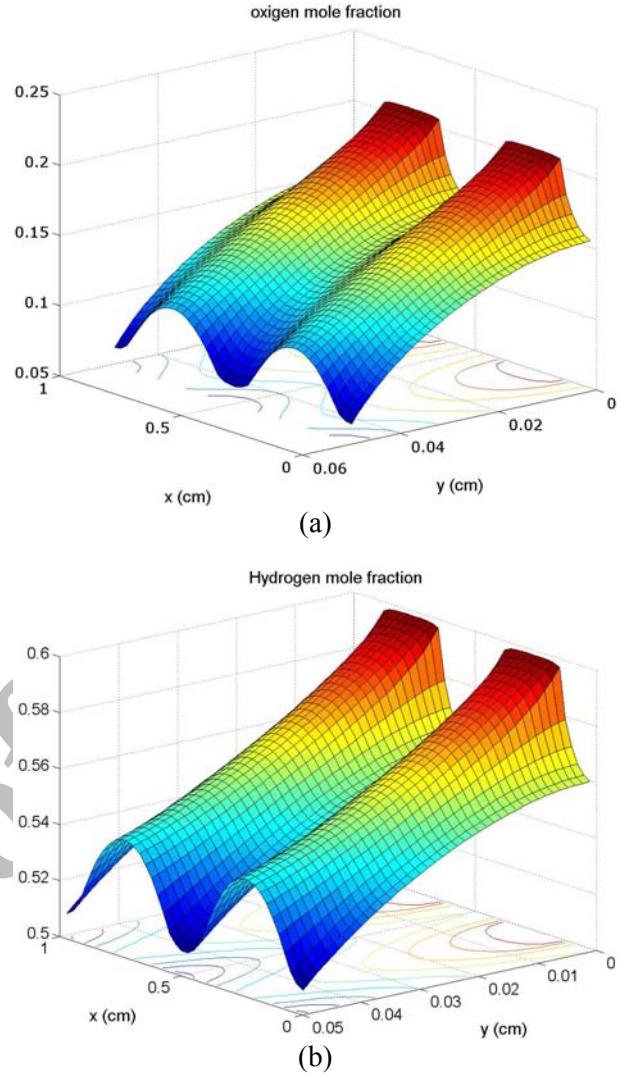

Figure 9. Reactant mole fraction in gas diffusion layer with consideration of compression effect and presence of water droplet on porosity of GDL (a) Cathode and (b) Anode side of cell.

layer. As a result, the variation of the produced electrical current increases across the electrodes. It means that some of the catalyst particles, especially under the landing area remain unused. If the variable catalyst loading (Apply more catalyst under channel where the reactant concentration is higher in this region) is taken into account, shown in Figure 12, the non-uniformity in the reactant concentration at GDL/catalyst layer interface might be diminished as shows in Figure 13.

In this case, the average electrical current density increases from 0.44 A/cm^2 to 0.5 A/cm^2. It is important to know if uniform and non uniform GDL porosity were compared with equal average porosity due to the fact that the results will not be identical. This is because of the non uniformity in produced electrical current in the catalyst layer could increase overpotentials in that layer. In addition in the case of non uniform porosity some catalyst particles remain unused because of the low concentration of the reactant which comes from the lower porosity in those

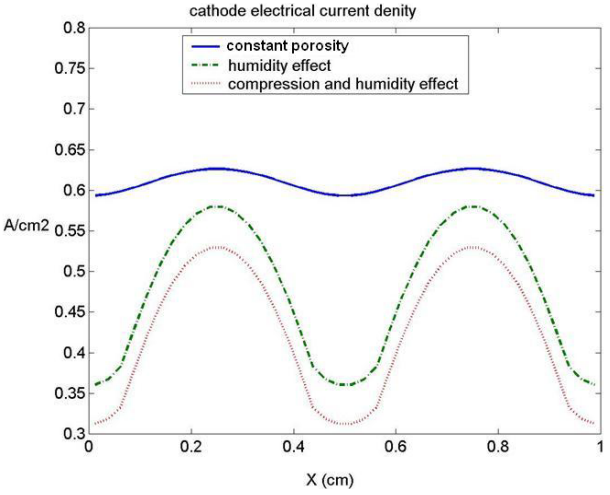

Figure 10. Electrical current density distribution in cathode side of a PEM fuel cell.

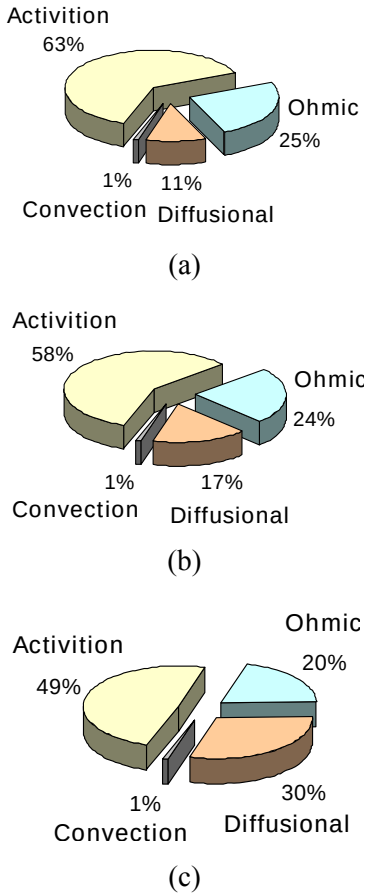

Figure 11. Percentage of overpotential contribution corresponding to (a) Constant porosity along GDL, (b) Spatial variation of porosity due to compression pressure and (c) Porosity as a function of water amount in GDL.

regions (under land areas which have a lower porosity due tocompression effect). Therefore the results due to the non-uniform porosity could match the results of the uniform one if the average porosity of the later (non uniform one) are lower. In other words, in case of non-uniform porosity, the average porosity could define in GDL and compare with the results with constant porosity.

Figure 14 presents the comparison of oxygen mole fraction in GDL/catalyst layer interface, with regular catalyst loading and with the variable catalyst loading applied to the catalyst layer. As can be seen from this figure the non-uniformity in oxygen mole fraction at GDL/catalyst interface could be substantially reduced by applying a variable catalyst loading.

4. CONCLUSION

The properties of the diffusion layer have a significant impact on the optimum performance of the catalyst and the electrodes. These layers are porous to allow for distribution of the gases to unexposed areas of the flow channel and this distribution allows for complete utilization of the electrode area. Many of simulations, have assumed, for simplicity, that the porosity of GDL is constant, but in practice, the compression pressure corresponding to the assembly process and presence of water in these layers may change the porosity distribution and affect gas diffusion coefficient in gas diffusion layers. Any change in porosity or diffusion coefficient can lead to a substantial influence on fuel cell performance owing to a diffusion overpotential change. The compression effect of GDLs and water generation due to the electrochemical reaction on the cathode side, also may cause non-uniformity in porosity and consequently in reactant concentration. Therefore, the produced electrical current has sharp gradient across the catalyst layer. If the variable catalyst loading is taken into account, the non-uniformity in the reactant concentration at GDL/catalyst layer interface might be diminished causing higher output voltage in polarization curve. Thus in order to achieve high cell performance, it is better to design and manufacture a non-uniform catalyst layer.

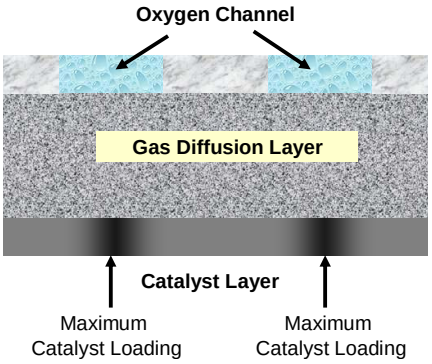

Figure 12. Variable catalyst loading (High catalyst loading under channels).

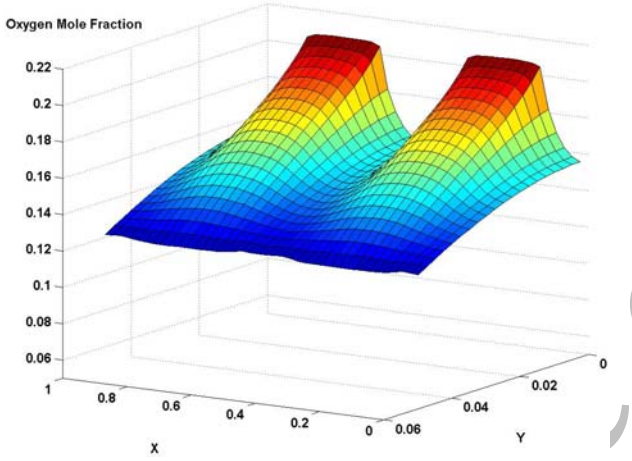

Figure 13. Oxygen mole fraction with variable catalyst loading (High catalyst loading under channels).

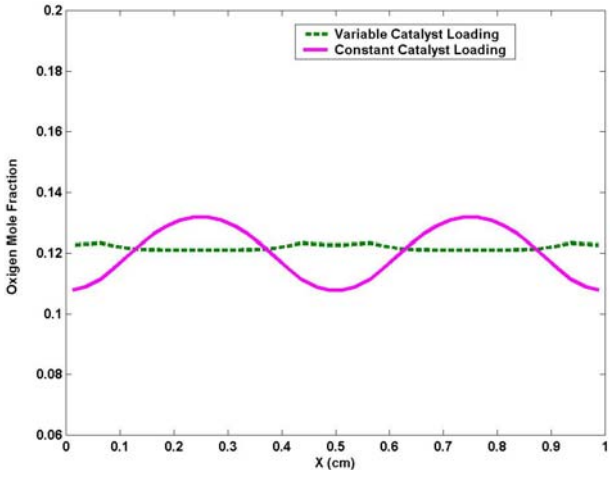

Figure 14. Histogram of the SSI for the signal represented in Figure 3: (a) Seizure activity, (b) Nonseizure activity.

5. NOMENCLATURE

A_V	Specific Area of Active Surface cm^{-1}
C	Concentration $mol.cm^{-3}$
$\overline{C}$	Channel Concentration $mol.cm^{-3}$
D	Diffusivity of Species cm^2/s
F	Faraday Constant C
H	Henry's Constant $atm.cm^3/mol$
I	Electrical Current A
i	Electrical Current Density A/cm^2
i_0	Exchange Electrical Current Density A/cm^2
K	Permeability cm^2
k_ϕ	Membrane Electro Kinetic Permeability cm^2
K_p	Membrane Hydraulic Permeability cm^2
l	Thickness cm
m	Molar Weight
M	Water Balance mol/s
n	Number of Electron Transferred in Reaction
N	Reactant Molar Flux mol/cm^2s
P	Pressure atm
R	Gas Constant J/mol°K
r_H	Catalyst Transfer Rate $cm.s^{-1}$
r_0	Channel/GDL Transfer Rate $cm.s^{-1}$
R_{cell}	Cell Resistance Ω
T	Temperature °K
U	Reactant Vlocity in GDL cm/s
V	Cell Potential Volt
w	Water Flux in Cell mol/cm^2s
x	Mole Fraction

Greek Letters

α	Transfer Coefficient
ε	porosity
ϕ	Potential Volt
δ	Water Density in Membrane Pores $mol.cm^{-3}$
η	Over Potentials Volt
κ	Ionic Conductivity 1/Ωcm
μ	Viscosity g/cms
ρ	Density g/cm^3
ω	Empirical Constant for Diffusion Overpotentials $\Omega cm^2/K$
σ	GDL Electrical Conductivity 1/Ωcm
ξ	Membrane Water Transport Ratio
ζ	Stoichiometric Ratio
∇	Gradient Operator

Subscripts

-	Anode
+	Cathode
act	Activation
c	Catalyst layer
conv	Convection
dif	Diffusion
g	Gas Diffusion Layer
h	Hydraulic
lim	Limitation
m	Membrane
max	Maximum Water Amount Corresponding to Complete Flooding
OCV	Open Circuit Voltage
ohm	Ohmic
S	Steady State Condition
w	Water
φ	Electro Kinetic

Superscripts

0	Initial Value
comp	Compression
eff	Effective Value
el	Electrochemical Reaction
hum	Humidity Condition
max	Maximum
out	Output
ref	Reference
s	Dissolve
sat	Saturation
tr	Transport

6. REFERENCES

1. Larminie, J. and Dicks, A., "Fuel cell system explained", John Willy and Sons, Ltd, (2000).
2. Thomas, S. and Zalbowitz, M., "Fuel cell green power", Los Alamos National Laboratory, New Mexico.
3. Hirschenhofer, J. H., Stauffer, D. B. and Engleman, R. "Fuel cells-a Hand book" (revision 3), U.S Department of Energy under contract No. DE-AC01-88FE61684, (1994).
4. Bernardi, D. M. and Verbrugge, M. W., "Mathematical model of the solid polymer electrolyte fuel cell", ***General motors report, GMR-7360***, Vol 15, (may, 1991).
5. Rowe, A. and Li, X., "Mathematical modeling of proton exchange membrane fuel cells", ***Journal of power sources***, Vol. 102, (2001), 82-96.
6. Thampan, T., Malhotra, S., Zhang, J. and Datta, R., "PEM fuel cell as a membrane reactor", ***Catalysis Today***, Vol. 67, (2001), 15-32.
7. Bernardi, D. M. and Verbrugge, M. W., "A mathematical model of the solid-polymer-electrolyte fuel cell", ***AIChE J***., Vol. 37, (1991), 1151-1163.
8. Dutta, S., Shimpalee, S. and Vanzee, J. W., "Numerical prediction of mass exchange between cathode and anode channels in a PEM fuel cell", ***International Journal of Heat and Mass Transfer***, Vol. 44, (2001) 2029-2042.
9. Um, S., Wang, C. Y. and Chen, K. S., "Computational fluid dynamic modeling of proton exchange membrane fuel cells", ***J. Electrochem. Soc***., Vol. 147, No. 12, (2000), 4485-4493.
10. Jordan, L. R., Shukla, A. K., Behrsing, T., Avery, N. R., Muddle, B. C. and Forsyth, M., ***Journal of Power sources***, Vol. 86, (2000), 250-254.
11. Jordan, L. R., Shukla, A. K., Behrsing, T., Avery, N. R., Muddle, B. C. and Forsyth, M., ***Journal of power sources***, Vol. 30, (2000), 641-646.
12. Giorgi, L., Antlini, E., Pozio, A. and Passalacaqua, E., ***Electrochem. Acta***, Vol. 43, (1998), 3675-3680.
13. Wohr, M., Bolwin, K., Schnurnbereger, W., Fischer, M., Neubrand, W. and Eigenberger, G., ***Int. J. Hydrogen Energy***, Vol. 23, (1998), 213-218.
14. Nam, J. H. and Kaviany, M., "Effective diffusivity and water-saturation distribution in single- and two-layer PEMFC diffusion medium", ***International Journal of Heat and Mass Transfer***, Vol. 46, (2003), 4595-4611.
15. Baschuk, J. J. and Li, X., "Modeling of polymer electrolyte membrane fuel cells with variable degrees of water flooding", ***Journal of power sources***, Vol. 181, (2000), 181-196.
16. Gurau, V., Barbir, F. and Liu, H., ***J.Elrctrochem. Soc***., Vol. 147, (2000), 4485-4493.
17. Chu, H. S., yeh, C. and Chen, F., "Effects of porosity change of gas diffuser on performance of proton exchange membrane fuel cell", ***Journal of power sources***, Vol. 123, (2003), 1-9.
18. Lee, W. K., Ho, C. H., Van Zee, J. W. and Murthy, M., "The effect of compression and gas diffusion layers on the performance of a PEM fuel cell", ***Journal of power sources***, Vol. 84, (1999), 45-51.
19. Zhan, Z., Xiao, J., Li, D., Pan, M. and Yuan, R., "Effects of porosity distribution variation on the liquid water flux through gas diffusion layers of PEM fuel cells", ***Journal of power sources***, Vol. 160, (2006), 1041-1048.
20. Lee, S., Hsu, C. and Huang, C., "Analysis of the fuel cell stack assembly pressure", ***Journal of power sources***, Vol. 145, (2005), 353-361.
21. Yan, W., Soong, C., Chen, F. and Chu, H., "Transient analysis of reactant gas transport and performance of PEM fuel cells", ***Journal of power source***, Vol. 143, (2005), 48-56.
22. Lin, H., Cheng, C. and Yan, W., "Optimization of key parameters in the proton exchange membrane fuel cell", ***Journal of power sources***, Vol. 162, (2006), 246-254.
23. Tao, W. Q., Min, C. H., Liu, X. L., He, Y. L., Yin, B. H. and Jiang, W., "Parameter sensitivity examination and discussion of PEM fuel cell simulation model

validation, Part I. Current status of modeling research and model development", ***Journal of power sources***, Vol. 160, (2006), 359-373.
24. Min, C. H., He, Y. L., Liu, X. L., Yin, B. H., Jiang, W. and Tao, W. Q., "Parameter sensitivity examination and discussion of PEM fuel cell simulation model validation, Part II. Results of sensitivity analysis and validation of the model", ***Journal of power sources***, Vol. 160, (2006), 374-385.
25. Ma, L., Ingham, D. B., Pourkashanian, M. and Carcadea, E., "Review of the computational fluid dynamic modeling of fuel cells", ***Journal of fuel cell science and technology***, Vol. 2, (November, 2005), 246-257.
26. Tobias, C. W., "Advances in Electrochemistry and Electrochemical Engineering", John Wiley, New York, (1962).
27. Stockie, J. M., Promislow, K. and Wetton, B. R., "A finite volume method for multi component gas transport in a porous fuel cell electrode", ***Int. J. Numerical Methods in Fluids***, (2001), 1-35.
28. Jeng, K. T., Lee, S. F., Tasi, G. F. and Wang, C. H., "Oxygen mass transfer in PEM fuel cell gas diffusion layers", ***Journal of Power sources***, Vol. 138, (2004), 41-50.
29. Maggio, G., Recupero, V. and Pino, L., "Modeling polymer electrolyte fuel cells", ***Journal of power sources***, Vol. 101, (2001), 275-286.
30. Berning, T., Liu, D. M. and Djilali, N., "Three-dimensional computational analysis of transport phenomena in a PEM fuel cell", ***Journal of Power Sources***, Vol. 106, (2002), 284-294.
31. Springer, T. E., Wilson, M. S., Gottesfeld, S., ***J. Elrctrochem. Soc***., Vol. 140, (1993), 3513-3525.
32. Oldhan, K. B. and Myland, J. C., "Fundamental of Electrochemical Science", ***Academic Press***, (1994).
33. Parthasarathy, A., Dave, B., Srinivasan, S., Appleby, J. A. and Martin, C. R., "The platinum microelectrode/Nafion interface: an electrochemical impedance spectroscopic analysis of oxygen reduction kinetics and Nafion characteristic", ***J. Electrochem. Soc***., Vol. 139, No. 6, 1634-1641.
34. Squadrito, G., Maggio, G., Passalacqua, E., Lufrano, F., Patti, A., ***J. Applied Electrochemistry***, Vol. 29, (1999), 1449-1455.
35. Salattery, J. C. and Bird, R. B., ***AlChE J***., Vol. 4, No. 137, (1988).
36. Nield, D. A., Bejan, A., "Convection in Porous media", ***second edition, Springer***, (1998).
37. Akanni, K. A., Evans, J. W. and Abramson, I. S., "Effective transport coefficients in heterogeneous media", ***Chem. Engrg. Sci***., Vol. 42, No. 8, (1987), 1945-1954.
38. Kolikovsky, A., "Numerical simulation of a new operational regime for a polymer electrolyte fuel cell", ***Electrochem. Communication***, Vol. 3, (2001), 460-466.